Journal of Quantitative Spectroscopy & Radiative Transfer 113 (2012) 2189–2196

Contents lists available at SciVerse ScienceDirect

Journal of Quantitative Spectroscopy & Radiative Transfer

journal homepage: www.elsevier.com/locate/jqsrt

Infrared absorption cross sections for methanol

Jeremy J. Harrison *, Nicholas D.C. Allen, Peter F. Bernath [1]

Department of Chemistry, University of York, Heslington, York YO10 5DD, United Kingdom

ARTICLE INFO

Article history:
Received 21 February 2012
Received in revised form
18 July 2012
Accepted 19 July 2012
Available online 27 July 2012

Keywords:
Methanol
High-resolution Fourier transform spectroscopy
Infrared absorption cross sections
Remote-sensing
Atmospheric chemistry

ABSTRACT

Infrared absorption cross sections for methanol, CH_3OH, have been determined near 3.4 and 10 μm from spectra recorded using a high-resolution FTIR spectrometer (Bruker IFS 125HR) and a multipass cell with a maximum optical path length of 19.3 m. Methanol/dry synthetic air mixtures were prepared and spectra were recorded at 0.015 cm^{-1} resolution (calculated as 0.9/MOPD) at a number of temperatures and pressures (50–760 Torr and 204–296 K) appropriate for atmospheric conditions. Intensities were calibrated using composite methanol spectra taken from the Pacific Northwest National Laboratory (PNNL) IR database. The new measurements in the 10 μm region indicate problems with the existing methanol spectroscopic line parameters in the HITRAN database, which will impact the accuracy of satellite retrievals.

1. Introduction

Methanol, the simplest of the organic alcohols, was first isolated in 1661 by Robert Boyle from the destructive distillation of boxwood [1]. Whereas the two-carbon analogue, ethanol, is a popular recreational drug, methanol is highly toxic to humans, causing blindness and/or death. Methanol is one of the main chemical commodities traded around the world, and is produced on an industrial scale, starting from synthesis gas, a mixture of CO and H_2, formed from the reaction of natural gas (principally CH_4) with steam or O_2. At high pressures, methanol is formed by the reaction of CO and H_2 over a catalyst (Cu and Zn/Mn/Al oxides).

Methanol is a common organic solvent, and is finding growing use [2] as a transportation fuel, a fuel additive, a hydrogen carrier in fuel cells, and in various processes such as biodiesel transesterification and wastewater denitrification. Its main use, however, is as a feedstock in the manufacture of other chemicals, including formaldehyde, (~ 40% of methanol supplies) and acetic acid. It also has important uses in the production of methyl methacrylate (MMA) and dimethyl terephthalate (DMT), both esters of methanol [1]. MMA is used in the manufacture of poly(methyl methacrylate) (PMMA), also known as Plexiglas or Perspex, used principally as a substitute for glass and also incorporated into paints, lacquers, enamels, and coatings. DMT is used in the manufacture of polyesters and plastics, e.g. polyethylene terephthalate (PET), used extensively in making plastic containers.

Methanol is not only important to our modern way of life, but also to interstellar chemistry because its formation provides a pathway to more complex organic molecules that are necessary for life. In the interstellar medium, methanol forms predominantly by successive hydrogenation of solid CO on the surfaces of dust grains [3]. Interstellar methanol was first discovered by Ball et al. in 1970 [4] in radio emission toward the galactic centre, and has since been detected in cometary atmospheres [5,6]. Empirical line intensities of methanol in the 300–500 cm^{-1} region

* Corresponding author. Tel.: +44 1904 324589; fax: +44 1904 322516.
E-mail address: jeremy.harrison@york.ac.uk (J.J. Harrison).
[1] Department of Chemistry and Biochemistry, Old Dominion University, Norfolk, VA, USA 23529.

0022-4073/$ - see front matter © 2012 Elsevier Ltd. All rights reserved.
http://dx.doi.org/10.1016/j.jqsrt.2012.07.021

have recently been obtained to support astronomical observations taken from orbit by the Heterodyne Instrument for Far Infrared (HIFI) instrument on the Herschel Space Observatory [7].

Closer to home, methanol is the second most abundant organic molecule in the Earth's atmosphere after methane [8], and its primary emissions contribute approximately 6% of the total terrestrial biogenic emissions of organic carbon [9]. According to Jacobs et al. [10], methanol emissions amount to 206 Tg yr^{-1}, arising from plant growth (62%), plant decay (11%), atmospheric oxidation of methane and other hydrocarbons (18%), biomass burning and biofuels (6%), and vehicles and industrial activities (2%).

The background concentration of methanol in the free troposphere ranges from ~0.4 to ~0.7 parts per billion (ppb) [11]. The main sink mechanism for methanol is oxidation by the OH radical to produce formaldehyde, HCHO. The effectiveness of this reaction is the primary reason for methanol's short lifetime, which is about one week [10].

Methanol has a negligible direct radiative forcing effect due to its short atmospheric lifetime. However, like many volatile organic compounds (VOCs) it has a significant impact on air quality and is implicated in the production of tropospheric ozone, which is toxic and a strong greenhouse gas. The 2007 IPCC report [12] lists tropospheric ozone as the third most important anthropogenic factor (after methane and carbon dioxide) in driving climate change. In the troposphere, methanol reacts with the OH radical, thereby lowering the amount of OH available to react with strong greenhouse gases such as CH_4; the result of this is to lengthen the CH_4 lifetime. Methanol, therefore, has an indirect contribution to radiative forcing; the 2007 IPCC report gives a calculated value of 2.8 for the indirect 100-year GWP (see Table 2.15 in Ref. [11]).

Increasingly satellite instruments are able to directly observe VOCs in the atmosphere. In particular, the Atmospheric Chemistry Experiment (ACE), on board SCISAT-1, currently detects more organic molecules than any other satellite instrument. The principal ACE instrument is a high-resolution Fourier transform spectrometer that covers the spectral region from 750 to 4400 cm^{-1} [13]. The ACE-FTS detected the first near global distribution of methanol in the upper troposphere (March 2004 to August 2005) [14]. Volume mixing ratios (VMRs) are typically about 0.5 ppb, but can be as high as 4.0 ppb in biomass burning plumes [15]. More recently the Tropospheric Emission Spectrometer (TES) [16] and the Infrared Atmospheric Sounding Interferometer (IASI) [17] have been able to detect enhanced methanol in the thermal infrared by nadir sounding [18]. TES and IASI offer superb global coverage (night and day) compared to ACE, but ACE has the advantage of providing vertical information.

Retrieving the concentrations of atmospheric species from satellite spectra require accurate laboratory spectroscopic measurements in the form of either line parameters or absorption cross sections. Currently v3.0 ACE methanol retrievals cover 5–25 km in altitude and make use of the spectroscopic line parameters in the HITRAN database [19], as derived by Xu et al. [20] in the 10 μm region; this band system is principally associated with the strong fundamental ν_8 mode at 1033 cm^{-1} (CO stretch) [21]. The 10 μm region of an ACE spectrum is dominated by saturated ozone lines, which limit the position of the principal retrieval microwindow to the region between 984.9 and 1005.1 cm^{-1}, at the edge of the band. On the other hand, retrieval microwindows for the nadir-viewing TES and IASI instruments cover the strong Q branch near 1033 cm^{-1}.

For the majority of the methanol 10 μm line parameters in HITRAN, the estimated line intensity uncertainties are in the range $\geq 10\%$ and $< 20\%$. The air-broadened (γ_{air}) and self-broadened (γ_{self}) half-widths were given assumed values of 0.1 and 0.4 cm^{-1} atm^{-1}, respectively, with the air-broadened pressure shift (δ_{air}) given a value of zero. Since the line parameters were derived from a set of room-temperature spectra, the coefficient (n_{air}) for the temperature dependence of γ_{air} was given an assumed value of 0.75. As these last four parameters have assumed values, HITRAN provides no indication of their errors. Uncertainties in all the spectroscopic line parameters [22], not just the line intensity, contribute to errors in the ACE methanol retrieval, but there is no simple way of knowing how γ_{air}, γ_{self}, n_{air}, and δ_{air} contribute to this overall error without performing laboratory measurements of the 10 μm band system at low temperature.

Typical errors in the ACE methanol VMRs are ~20–30% [14]. In order to improve the accuracy of ACE retrievals, new spectroscopic data for the methanol band near 3.4 μm, which lies in a less-congested region of the spectrum, have been obtained in the form of absorption cross sections over a range of pressures and temperatures (50–760 Torr and 204–296 K). Currently the HITRAN database contains no data in this spectral region, largely because of the difficulties in making unambiguous assignments for individual lines; the most intense spectral lines in this region are densely packed into an interval of ~500 cm^{-1}. This band system is associated with three CH stretch fundamental modes, ν_3 at 2844 cm^{-1} (symmetric), ν_2 at 3000 cm^{-1} and ν_9 at 2960 cm^{-1} (both asymmetric). There have been a number of efforts to model and quantify the CH stretch region of methanol [23–25]; most recently, a new line-by-line model for the ν_3 band has been constructed [26].

Ideally, in the future ACE retrievals will make use of both absorption bands at 3.4 and 10 μm, so it is crucial that the intensities for these two regions are consistent. Additional measurements have been made in the 10 μm region over a range of pressures and temperatures (50–760 Torr and 204–296 K) to compare with the existing HITRAN data. This work provides the first low temperature quantitative measurements of methanol for atmospheric remote-sensing purposes. Such measurements are difficult because methanol has a low vapour pressure at low temperatures (~1.0 Torr at 230 K and ~0.05 Torr at 203 K) [27], so that long optical pathlengths must be used for spectroscopic measurements in order to achieve sufficient signal-to-noise ratios.

2. Air-broadened spectral measurements of methanol

Air-broadened methanol absorption spectra were recorded at the Molecular Spectroscopy Facility (MSF), Rutherford Appleton Laboratory (located in Oxfordshire,

UK), using a Bruker Optics IFS 125HR high-resolution Fourier transform spectrometer (FTS) with an internal mid-infrared radiation source (globar). A calcium fluoride (CaF_2) beamsplitter and indium antimonide (InSb) detector were utilised for measurements near 3.4 μm, with a potassium bromide (KBr) beamsplitter and a mid-band mercury cadmium telluride (MCT) detector used for measurements near 10 μm. The FTS was set to a resolution of 0.015 cm^{-1} (calculated as the Bruker instrument resolution of 0.9/MOPD), with suitable optical filters and the aperture diameter (2.5 mm) chosen so that the intensity of infrared radiation falling on the detectors was maximised in the spectral region of interest without saturation or loss of spectral resolution. Norton–Beer weak apodisation and Mertz phase corrections were applied to all interferograms. Due to the non-linear response of MCT detectors to the detected radiation, which results in baseline perturbations, all interferograms measured using the MCT detector were re-transformed using the non-linearity correction in Bruker's OPUS software. The FTS instrumental parameters and settings are summarised in Table 1.

The vapour pressure of methanol at low temperatures is very small, so spectral measurements require long pathlengths to compensate. For this reason, this work makes use of the MSF short-path absorption cell (SPAC), which has previously been used for acetone [28,29] and acetonitrile [30,31] measurements. The SPAC, so-named to distinguish it from the LPAC which has an even longer pathlength capability, is a coolable, multipass White cell, with two externally adjustable mirrors, capable of achieving an optical pathlength between 1.7 m and 19.3 m (in steps of 1.6 m). In these experiments the SPAC was operated from room temperature down to 204 K. For each measurement, the actual cell temperature (which can be automatically controlled for extended periods of time) was monitored by six platinum resistance thermometers situated at positions throughout the inner sample vessel

Table 1
FTS and SPAC configurations.

	SWIR (3.4 μm)	LWIR (10 μm)
Detector	Indium antimonide (InSb)	Mercury cadmium telluride (MCT)
Beam splitter	Calcium fluoride (CaF_2)	Potassium bromide (KBr)
Optical filter	F754 (Northumbria Optical Coatings Ltd.) ~2600–3300 cm^{-1} bandpass	LP 5.75 μm (Northumbria Optical Coatings Ltd.) ~800–1700 cm^{-1} bandpass
Source	Globar (mid infrared)	
Resolution	0.015 cm^{-1}	
Aperture size	2.5 mm	
Apodisation function	Norton–Beer weak	
Phase correction	Mertz	
Cell windows	Barium fluoride (BaF_2)	
Transfer optics chamber windows	Potassium bromide (KBr)	
Mirror coatings	Gold	
Pressure gauges	3 MKS-690A Baratrons (1, 10 and 1000 Torr) (±0.05% accuracy)	
Thermometry	6 PRTs, Labfacility IEC 751 Class A	

of the SPAC. The sample pressure in the cell was measured by three MKS-690A Baratron capacitance manometers (full scale 1, 10 and 1000 Torr) connected to the gas line, close to the SPAC inlet.

Methanol (Merck Uvasol, ≥99.9% purity) was purified to remove dissolved air using multiple freeze–pump–thaw cycles with liquid N_2. A small amount of cold methanol vapour was introduced into the sample cell from a small glass tube via a gas-handling line, which was connected to a turbomolecular vacuum pump to evacuate the line and cell between measurements. Sample mixtures were prepared by adding dry synthetic air ('Air Zero Plus', Air Products, 99.99990% overall purity; used without additional purification) to the methanol vapour.

Details of the pressures, temperatures, optical pathlengths, and the number of scans taken for each sample are contained in Table 2. Additionally, evacuated-cell background scans were recorded before and after the scan blocks for each sample, and scans of pure nitrous oxide (N_2O) were recorded at each temperature to calibrate the frequency scale. The temperatures and pressures of the sample mixtures were logged by computer every few seconds. The variations in these quantities were used to estimate their experimental uncertainties (see Table 2).

3. Determination of absorption cross sections for methanol

Transmittance spectra were calculated by dividing averaged single-channel sample scans by appropriate averaged single-channel background scans. Channel fringes were observed in all scans, but these normally cancelled when transmittance spectra were calculated. When they did not cancel exactly, the method outlined previously for acetone/acetonitrile measurements [28–31] was used to remove these fringes. Once transmittance spectra were calculated, a small baseline correction was sometimes necessary to account for small signal drifts between single-channel sample and background scans.

Spectral frequencies were calibrated using pure N_2O spectra recorded during the experimental run. The positions of isolated N_2O absorption lines, in the ranges 1140–1320 cm^{-1} and 2780–2820 cm^{-1} were taken from the HITRAN 2008 database [19]. The wavenumber accuracy of the methanol measurements is comparable to the accuracy of the selected N_2O lines, which is between 0.001 and 0.0001 cm^{-1}.

Spectral absorption cross sections, $\sigma(\upsilon,P_{air},T)$, with units cm^2 $molecule^{-1}$, were calculated using the equation

$$\sigma(\upsilon,P_{air},T) = -\xi \frac{10^4 k_B T}{Pl} \ln\tau(\upsilon,P_{air},T) \quad (1)$$

where $\tau(\upsilon,P_{air},T)$ is the transmittance at wavenumber υ (cm^{-1}), temperature T (K) and synthetic air pressure P_{air}, P is the pressure of the absorbing gas (Pa), l is the optical pathlength (m), k_B is the Boltzmann constant ($=1.3806504\times10^{-23}$ $J\,K^{-1}$), and ξ is a normalisation factor to account for the difficulty in accurately determining the absorber amount in the cell. (This procedure makes the assumption that the integrated band intensity in each spectral region is invariant to temperature. A full

Table 2
Summary of the sample conditions for all scans.

	Temperature (K)	Initial methanol pressure (Torr)[a]	Total pressure (Torr)	Pathlength[b] (m)	No. of scans[c]
SWIR (3.4 μm)	204.5 ± 0.7	0.0137	50.92 ± 0.10	19.31	320
	204.3 ± 0.4	0.0137	75.82 ± 0.10	19.31	322
	204.4 ± 0.4	0.0137	101.62 ± 0.10	19.31	380
	214.2 ± 0.9	0.0531	50.52 ± 0.10	19.31	300
	214.2 ± 0.8	0.0562	102.67 ± 0.15	19.31	286
	214.3 ± 0.9	0.0560	260.0 ± 0.4	19.31	244
	248.1 ± 1.0	0.4924	205.3 ± 0.3	3.31	300
	247.8 ± 1.0	0.5080	402.5 ± 0.5	3.31	300
	247.8 ± 1.0	0.5051	600.3 ± 0.6	3.31	300
	272.1 ± 0.6	0.5001	369.6 ± 0.4	3.31	400
	272.3 ± 0.7	0.5169	600.1 ± 0.6	3.31	400
	296.0 ± 0.2	0.8210	760.8 ± 0.2	1.71	350
LWIR (10 μm)	204.0 ± 0.8	0.0107	50.17 ± 0.10	19.31	200
	203.9 ± 0.8	0.0107	74.97 ± 0.10	19.31	300
	203.9 ± 0.9	0.0107	98.54 ± 0.15	19.31	300
	219.2 ± 1.1	0.0166	49.95 ± 0.10	19.31	300
	219.4 ± 1.2	0.0166	99.35 ± 0.15	19.31	300
	219.5 ± 1.0	0.0130	249.2 ± 0.8	19.31	280
	249.0 ± 0.6	0.1881	201.7 ± 0.2	1.71	400
	249.4 ± 0.7	0.1864	400.7 ± 0.5	1.71	300
	249.2 ± 0.7	0.1924	604.4 ± 0.6	1.71	300
	273.1 ± 1.0	0.2392	369.7 ± 0.4	1.71	300
	272.9 ± 0.9	0.2293	599.7 ± 0.8	1.71	300
	295.4 ± 0.2	0.2872	761.3 ± 0.2	1.71	300

[a] MKS-690A Baratron readings are accurate to ± 0.05%.
[b] The error in the optical pathlength is estimated to be ± 0.2% at room temperature.
[c] Note that each sample requires the measurement of a similar number of background scans taken with the same spectrometer settings. One scan takes about 33 s.

justification for this is presented in Section 4.) The methanol partial pressures cannot be monitored throughout the measurements in the same manner as the total pressures, so the initial pressures (before the addition of synthetic air) are used for P, the pressure of the absorbing gas, in Eq. (1). When methanol vapour is first added to the cell, some of it condenses on the cold metal surfaces. The addition of warm synthetic air initially leads to a slight increase in temperature followed by a decrease as this additional gas provides a more efficient cooling pathway to achieve thermal equilibrium. The subsequent small readjustment in cell temperature can lead to changes in methanol vapour pressure, which has the largest effect at the lowest temperatures. This change in pressure is difficult to quantify, but generally the actual amount of absorber present in the cell during a measurement is smaller than the initial pressure, especially at low temperature, i.e. ξ is above 1. The values of ξ were determined by normalising the absorption cross sections using the following relationships:

$$\int_{877\ \mathrm{cm^{-1}}}^{1177\ \mathrm{cm^{-1}}} \sigma(\upsilon,P_{\mathrm{air}},T) = 1.841 \times 10^{-17}\ \mathrm{cm\ molecule^{-1}}(\pm 0.1\%) \quad (2)$$

$$\int_{2600\ \mathrm{m^{-1}}}^{3250\ \mathrm{cm^{-1}}} \sigma(\upsilon,P_{\mathrm{air}},T) = 2.127 \times 10^{-17}\ \mathrm{cm\ molecule^{-1}}(\pm 0.1\%) \quad (3)$$

The values on the right hand sides of Eqs. (2) and (3) are the average integrated band strengths of two Pacific Northwest National Laboratory (PNNL) methanol spectra (recorded at 278 and 298 K) in the ranges 877–1177 $\mathrm{cm^{-1}}$ and 2600–3250 $\mathrm{cm^{-1}}$, respectively, converted from PNNL units ($\mathrm{ppm^{-1}\,m^{-1}}$ at 296 K) using the factor $k_B \times 296 \times \ln 10 \times 10^4/0.101325$. The uncertainty in parentheses represents the spread from the mean of the two PNNL integrated band intensities for each spectral range. Note that the integrated band strength at 323 K is ~2% lower than at the other two temperatures. The reason for this is unknown, but since the measurement was made at a higher temperature than any of the measurements reported in this work, it was decided not to include it in the average calculation.

The choice of using low-resolution, 760 Torr N_2-broadened methanol spectra from the PNNL IR database (http://nwir.pnl.gov) [32] as accurate intensity standards was taken for a number of reasons. Each PNNL spectrum is a composite of multiple pathlength–concentration burdens, and great care has been taken to ensure that sample concentrations have been determined accurately. Once normalised, the two new methanol cross sections at ~296 K and ~760 Torr agree very well with the PNNL spectrum at 298 K and 760 Torr; the higher resolution of the present measurements results in slightly sharper spectral features.

As mentioned earlier, these cross sections cover a number of methanol vibrational band systems. The 10 μm band system is associated with the strong fundamental mode ν_8 (CO stretch) [21], whereas the congested 3.4 μm band system is associated with three CH stretch fundamental modes, ν_3, ν_2 and ν_9. Both spectral regions

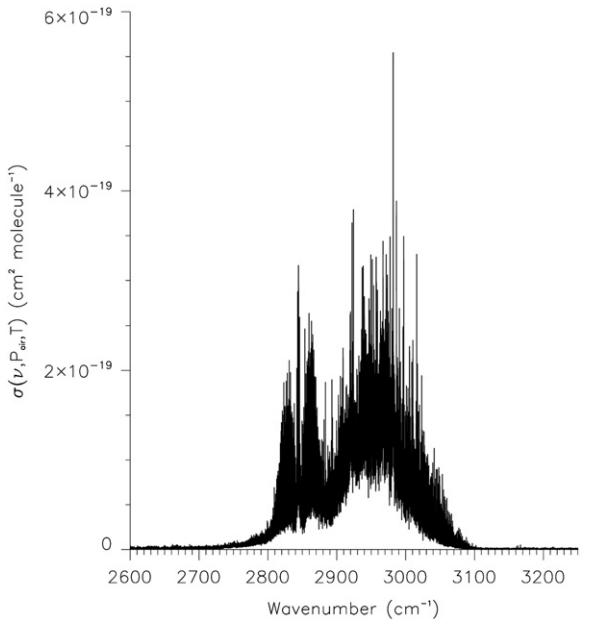

Fig. 1. Methanol absorption cross section near 3.4 μm at 204.5 K and 50.92 Torr.

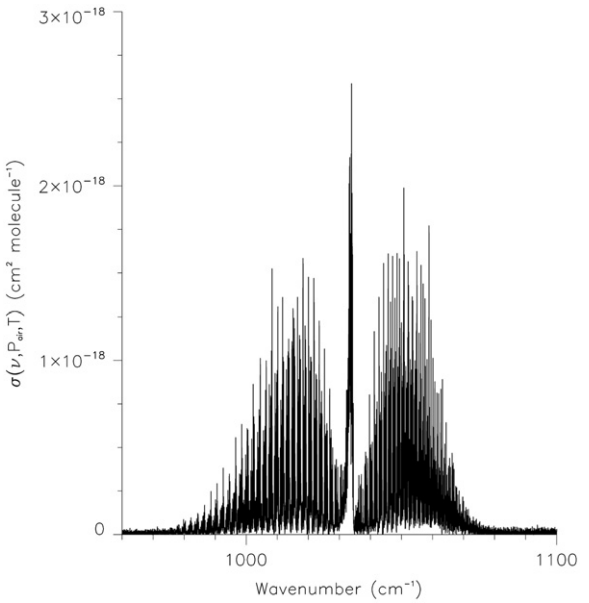

Fig. 2. Methanol absorption cross section near 10 μm at 204.0 K at 50.17 Torr.

also contain numerous combination and overtone bands. Figs. 1 and 2 provide plots of the absorption cross sections at ~204 K and ~50 Torr in the 3.4 μm and 10 μm regions, respectively.

In principle, one could obtain an estimate of the random errors by taking many measurements at each temperature and (broadening) pressure combination, as is the case for measurements in the PNNL IR database. However, we do not do this; a measurement is taken at one methanol concentration for each pressure - temperature combination due to time constraints and the need to maximise the signal-to-noise at the longest pathlengths. Uncertainties in the sample temperatures and total pressures range from 0.07 to 0.5% and 0.03 to 0.3%, respectively (Table 2). The photometric uncertainty is estimated to be 1–2%. The pathlength error at room temperature is estimated to be 0.2%, increasing slightly as the cell is cooled because the mirrors and optical components change position as they contract. The exact temperature dependence of the systematic error this introduces into the optical pathlength at low temperatures has not been quantified, but should be small; it is accounted for by normalising against PNNL methanol spectra, which have a stated experimental accuracy of 1.5% (1σ). We estimate an overall uncertainty in the new methanol cross sections of 5% (1σ).

This set of spectral absorption cross sections for methanol are available electronically upon request from the authors, and will be made available to the community via the HITRAN database.

4. Justification for the assumed temperature invariance of the integrated band intensity

As mentioned in the previous section, the normalisation procedure assumes that the integrated intensity over each band system is independent of temperature. This assumption is a good one for isolated bands comprising primarily fundamentals [33,34], and has been used successfully for past measurements. However, the methanol spectrum contains complex hot-band and overtone structure, due to the low-energy torsional energies near ~300 cm^{-1}; the contribution of hot bands to the spectrum at 296 K is estimated to be 33% [26]. The presence of overtone, combination and hot bands can introduce a small temperature dependence to the overall integrated band intensity. In order to check the validity of this approximation for methanol, additional spectra were recorded for pure samples over a number of temperatures. By using pure methanol samples, it was possible to monitor absorber pressures throughout the scans, unlike for the air-broadened measurements. Ideally, pure spectra should be recorded at very high resolution determined by the Doppler linewidth, however this was not possible due to the lack of time available to record the large number of scans necessary to obtain adequate signal-to-ratio ratios. Instead, it was decided to record spectra at lower spectral resolution, thus allowing the aperture diameter to be increased, shortening the scans, and improving the signal-to-noise. Methanol pressures were chosen such that the Doppler-resolved lines would not be saturated if they were to be recorded at very high resolution (~0.002 cm^{-1}), otherwise errors would be introduced into the derived band intensities when recorded at lower resolution.

Spectra of the band near 3.4 μm were recorded for various temperatures between 214 and 293 K at a resolution of 0.0225 cm^{-1} (MOPD=40 cm, aperture diameter=3.15 mm) and 171 cm pathlength. Spectra for the 10 μm band were recorded for a number of temperatures between 212 and 296 K at resolutions of 0.0225 cm^{-1}

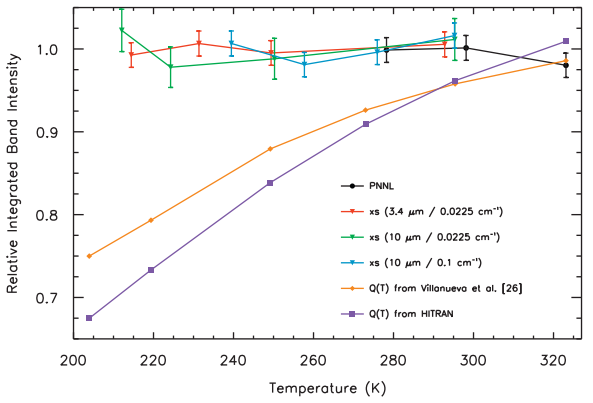

Fig. 3. Integrated band intensities for the three composite PNNL spectra (the average of those at 278 K and 298 K is given a value of one), compared with the relative band intensities for the low-resolution, pure measurements described in Section 4. Also plotted are relative band intensities from simulations using HITRAN line parameters in the 10 μm region; partition sums come from two sources: the HITRAN database file "parsum.dat" and the new data from Villanueva et al. [26].

(aperture diameter=5 mm) and 0.1 cm^{-1} (MOPD=9 cm, aperture diameter=5 mm), and pathlengths 171 and 26 cm, respectively. The chosen methanol pressures resulted in absorptances of the order of 40–50%, 25–30%, and 10–15%, respectively. The signal-to-noise obtained for the 10 μm/0.0225 cm^{-1} spectra created difficulties in positioning the spectral baselines. For this reason additional measurements were taken at lower resolution (0.1 cm^{-1}) using a short pathlength cell, providing better overall signal-to-noise.

Integrated band intensities for the three composite PNNL spectra (at 278, 298 and 323 K) are plotted in Fig. 3; the average of those at 278 K and 298 K is given a value of one; note that these values are the same for each band. These three PNNL data points provide no support for any temperature dependence in the range 278–323 K. Superimposed on Fig. 3 are the relative band intensities for the pure measurements (absorption cross sections were calculated using Eq. (1) with ξ set to 1). These integrated band intensities do not provide any evidence for temperature dependence, although, due to experimental error, a small dependence of the order of 2 or 3% cannot be ruled out. Note that it was anticipated that these lower resolution measurements would provide a simple means of investigating the temperature dependence of the band strength, however they do not provide accurate absolute band intensities. For example, a synthetic pure methanol spectrum calculated at 296 K and 0.1 cm^{-1} resolution using HITRAN line parameters gives an integrated band intensity ~10% lower than that calculated at 296 K and air-broadened to 760 Torr. Therefore, to adjust for the variation in absolute intensity, the three datasets (3.4 μm/0.0225 cm^{-1}, 10 μm/0.0225 cm^{-1} and 10 μm/0.1 cm^{-1}) have been adjusted by 2%, 15%, 10%, respectively, in order to better agree with the PNNL values. The large adjustment for the second dataset, with the poorest signal-to-noise, is due to the difficulty in determining the true baseline.

5. Comparison with simulations using HITRAN line parameters (10 μm)

Simulated methanol spectra using HITRAN line parameters in the 10 μm region and partition sums from the file "parsum.dat", which is distributed with the HITRAN database, reveal a significant temperature dependence in the integrated band intensity, which drops 30% from 296 to 204 K. There is no information in the database as to how these partition sums were calculated. When using the new partition sums from Villanueva et al. [26], this temperature dependence is less pronounced; the band intensity drops only 22% from 296 to 204 K. The values from Villanueva et al. agree well (~0.2%) with those from Pearson and Xu [26], who used a different approach in the computations, and should be the most suitable for spectral simulations at the temperatures presented in this work; this points to a problem with the HITRAN values. Relative band intensity values for the two cases are plotted for a number of temperatures in Fig. 3. Integrated band intensities from the low resolution, pure methanol spectra and the three composite PNNL spectra (also presented in Fig. 3) do not support the temperature dependence of the integrated band strengths calculated using HITRAN, suggesting a problem with the HITRAN line parameters.

Note that the PNNL band intensities are ~5% higher than those calculated from HITRAN at room temperature. This is due to differences in the baseline, weak lines missing from the HITRAN database, and line parameter errors. Fig. 4 illustrates this clearly by superimposing the air-broadened laboratory transmittance spectrum at 295.4 K (refer to Table 2 for full sample conditions) with the corresponding synthetic spectrum. Considering the difficulty in assigning lines in such a complex spectral region, it is unsurprising that the agreement is not ideal.

Even after scaling the band intensities of the synthetic spectra (at 10 μm) to better match the absorption cross sections for the lowest temperatures, differences remain. It is expected that the new, low temperature measurements provide a higher level of accuracy because the HITRAN line intensity uncertainties are in the range ≥10% and <20%, and other lineshape parameters, for

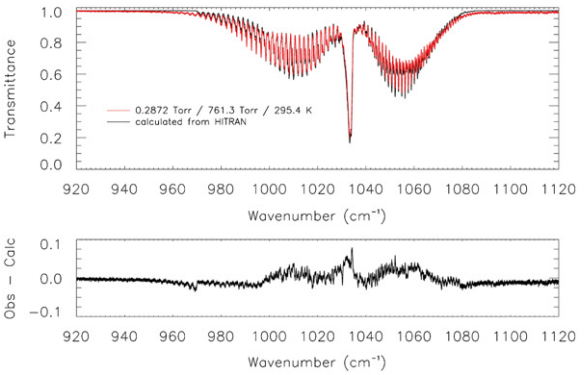

Fig. 4. Comparison between the air-broadened laboratory transmittance spectrum (10 μm) of methanol at 295.4 K (0.2872 Torr methanol, 761.3 Torr total pressure) with the corresponding synthetic spectrum calculated using the HITRAN linelist.

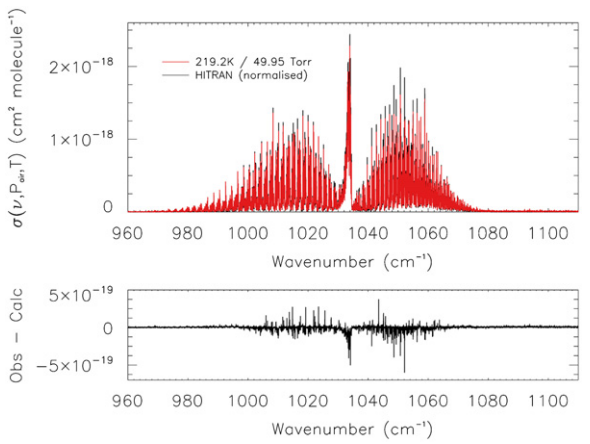

Fig. 5. Comparison between the methanol absorption cross section (10 μm) at 219.1 K and 49.95 Torr, and that calculated using the HITRAN linelist.

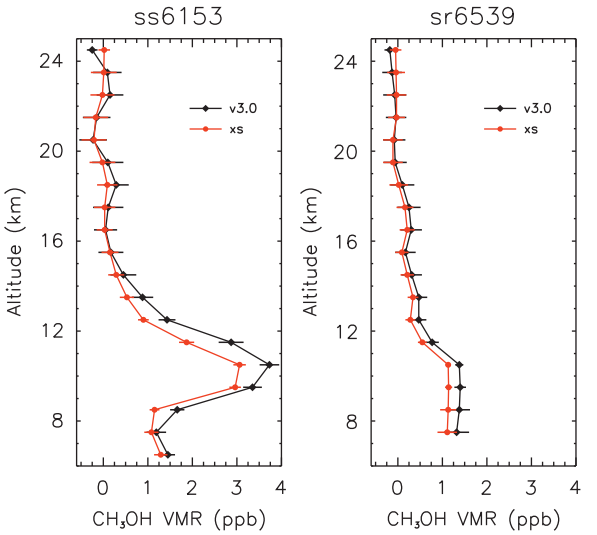

Fig. 6. Comparison between ACE profiles using the new methanol cross sections (10 μm only) and the v3.0 data product for occultations ss6153 and sr6539.

example the coefficient for the temperature dependence of the air-broadened half-width, have assumed values. Fig. 5 provides a comparison between the cross section at 219.1 K and 49.95 Torr, and a synthetic, normalised spectrum calculated using HITRAN.

It is not entirely clear where the problem with the HITRAN calculations lies. Although the partitions sums provided with HITRAN are incorrect, those provided by Villanueva [26] are expected to be good over the temperature range of the measurements presented in this work (<300 K). The other possibility is the methanol linelist itself. As outlined by Xu et al. [20], the derivation of the HITRAN linelist was rather difficult and it is not ideal. The ν_8 band was modelled using an isolated-band approach without vibrational interactions. However, this approach did not reproduce the spectrum within experimental error. Many combination and overtone bands have visible intensity in the spectrum; many of these are perturbation-induced or gain intensity via anharmonic and Coriolis interactions with ν_8, and cannot be modelled using an isolated-band approach. These weaker lines were simply given empirical positions and intensities in the linelist. For the final HITRAN linelist, calculations were merged with observed positions and intensities where possible. However, the observed intensity does not necessarily correspond to the assigned transition if underlying contributions from weaker combination and hot bands have not been accurately taken into account.

It is hoped that the new measurements presented in this work will generate renewed interest in improving the methanol line parameters in HITRAN.

6. ACE retrievals

The choice to normalise all cross sections to the same value is expected to provide a more accurate basis for retrieving methanol abundances from atmospheric IR spectra recorded by satellite instruments, e.g. the ACE-FTS. ACE methanol v3.0 retrievals use partition function data from the HITRAN database file "parsum.dat". Based on the previous arguments, it is expected that retrievals using the new cross sections will give slightly lower VMRs. Indeed, this is observed. Fig. 6 provides a comparison between ACE profiles using the new methanol cross sections (10 μm only) and the v3.0 profiles for occultations ss6153 and sr6539. The forward models differ only in the source of methanol spectroscopy. These occultations were included in the first publication detailing ACE measurements of methanol [15], which focussed on enhancements inside aged southern tropical to mid-latitude biomass burning plumes during October 2004; occultation ss6153 is located east of South Africa, with sr6539 north of New Zealand. It is anticipated that the absorption cross sections in the 3 μm region will improve the ACE methanol retrieval and provide more accurate background concentrations.

7. Conclusions

High-resolution infrared absorption cross sections for methanol (in the 3.4 and 10 μm regions) have been determined with an estimated uncertainty of 5%. Spectra were recorded for mixtures of methanol with dry synthetic air at 0.015 cm^{-1} resolution (calculated as 0.9/MOPD) over a range of temperatures and pressures appropriate for UTLS conditions and a multipass cell with a maximum optical pathlength of 19.3 m. Intensities were calibrated against methanol spectra in the PNNL IR database. These cross sections will enable retrievals of methanol from atmospheric spectra recorded by IR remote sensing instruments on board satellites, such as the ACE-FTS. The new measurements in the 10 μm region indicate problems with the existing methanol spectroscopic line parameters in the HITRAN database, which will impact the accuracy of satellite retrievals. Until these problems are resolved, it is recommended that future retrievals make use of these new data.

Acknowledgements

The authors wish to thank the Natural Environment Research Council (NERC) for supporting J.J. Harrison through Grants NE/F002041/1 and NE/I022663/1, as well as N.D.C. Allen through the National Centre for Earth Observation (NCEO), and for access to the Molecular Spectroscopy Facility (MSF) at the Rutherford Appleton Laboratory (RAL). R.G. Williams and R. McPheat are thanked for providing technical support at the RAL. C.D. Boone is thanked for providing software to simulate spectra from HITRAN line parameters. The ACE satellite mission is funded primarily by the Canadian Space Agency.

References

[1] Myers RL. The 100 most important chemical compounds: a reference guide. Westport, Connecticut, USA: Greenwood Press; 2007.
[2] 〈http://www.methanol.org/〉 [accessed February 2012].
[3] Whittet DCB, Cook AM, Herbst E, Chiar JE, Shenoy SS. Observational constraints on methanol production in interstellar and preplanetary ices. Astrophys J 2011;742:28. http://dx.doi.org/10.1088/0004-637X/742/1/28.
[4] Ball JA, Gottlieb CA, Lilley AE, Radford HE. Detection of methyl alcohol in sagittarius. Astrophys J 1970;162:L203–10.
[5] Bockelée-Morvan D, Colom P, Crovisier J, Despois D, Paubert G. Microwave detection of hydrogen sulphide and methanol in comet Austin (1989c1). Nature 1991;350:318–20. http://dx.doi.org/10.1038/350318a0.
[6] Bockelée-Morvan D, Brooke TY, Crovisier J. On the origin of the 3.2- to 3.6 μm emission features in comets. Icarus 1995;116:18–39.
[7] Brauer CS, Sung K, Pearson JC, Brown LR, Xu L-H. Empirical line intensities of methanol in the 300–500 cm^{-1} region. J Quant Spectrosc Radiat Transfer 2012;113:128–39.
[8] Singh HB, Chen Y, Staudt A, Jacob D, Blake D, Heikes B, et al. Evidence from the Pacific troposphere for large global sources of oxygenated organic compounds. Nature 2001;410:1078–81.
[9] Heikes B, Chang W, Pilson MEQ, Swift E, Singh HB, Guenther A, et al. Atmospheric methanol budget and ocean implication. Global Biogeochem Cycles 2002;16:1133. http://dx.doi.org/10.1029/2002GB001895.
[10] Jacob DJ, Field BD, Li Q, Blake DR, de Gouw J, Warneke C, et al. Global budget of methanol: constraints from atmospheric observations. J Geophys Res 2005;110:D08303. http://dx.doi.org/10.1029/2004JD005172.
[11] Singh HB, Kanakidou M, Crutzen PJ, Jacob DJ. High concentrations and photochemical fate of oxygenated hydrocarbons in the global troposphere. Nature 1995;378:50–4.
[12] IPCC. Climate Change. The physical science basis. In: Solomon S, Qin D, Manning M, Chen Z, Marquis M, Averyt KB, Tignor M, Miller HL, editors. Contribution of working group i to the fourth assessment report of the intergovernmental panel on climate change. Cambridge, United Kingdom and New York, NY, USA: Cambridge University Press; 2007 〈http://www.ipcc.ch/〉.
[13] Bernath PF, McElroy CT, Abrams MC, Boone CD, Butler M, Camy-Peyret C, et al. Atmospheric chemistry experiment (ACE): mission overview. Geophys Res Lett 2005;32:L15S01, http://dx.doi.org/10.1029/2005GL022386.
[14] Dufour G, Szopa S, Hauglustaine DA, Boone CD, Rinsland CP, Bernath PF. The influence of biogenic emissions on upper-tropospheric methanol as revealed from space. Atmos Chem Phys 2007;7:6119–29.
[15] Dufour G, Boone CD, Rinsland CP, Bernath PF. First space-borne measurements of methanol inside aged southern tropical to mid-latitude biomass burning plumes using the ACE-FTS instrument. Atmos Chem Phys 2006;6:3463–70.
[16] Beer R, Shephard MW, Kulawik SS, Clough SA, Eldering A, Bowman KW, et al. First satellite observations of lower tropospheric ammonia and methanol. Geophys Res Lett 2008;35:L09801. http://dx.doi.org/10.1029/2008GL033642.
[17] Coheur P-F, Clarisse L, Turquety S, Hurtmans D, Clerbaux C. IASI measurements of reactive trace species in biomass burning plumes. Atmos Chem Phys 2009;9:5655–67. http://dx.doi.org/10.5194/acp-9-5655-2009.
[18] Wells KC, Millet DB, Hu L, Cady-Pereira KE, Xiao Y, Shephard MW, et al. Tropospheric methanol observations from space: retrieval evaluation and constraints on the seasonality of biogenic emissions. Atmos Chem Phys Discuss 2012;12:3941–82, http://dx.doi.org/10.5194/acpd-12-3941-2012.
[19] Rothman LS, Gordon IE, Barbe A, Benner DC, Bernath PF, Birk M, et al. The HITRAN 2008 molecular spectroscopic database. J Quant Spectrosc Radiat Transfer 2009;110:533–72.
[20] Xu L-H, Lees RM, Wang P, Brown LR, Kleiner I, Johns JWC. New assignments, line intensities, and HITRAN database for CH_3OH at 10 μm. J Mol Spectrosc 2004;228:453–70.
[21] Shimanouchi T, 2005. Molecular vibrational frequencies. In: Linstrom PJ, Mallard WG, editors. NIST Chemistry WebBook, NIST Standard Reference Database Number 69. Gaithersburg, MD 20899: National Institute of Standards and Technology. 〈http://webbook.nist.gov/〉.
[22] Harrison JJ, Bernath PF, Kirchengast G. Spectroscopic requirements for ACCURATE, a microwave and infrared-laser occultation satellite mission. J Quant Spectrosc Radiat Transfer 2011;112:2347–54. http://dx.doi.org/10.1016/j.jqsrt.2011.06.003.
[23] Hunt RH, Shelton WN, Cook WB, Bignall ON, Mirick JW, Flaherty FA. Torsion-rotation absorption line assignments in the symmetric CH-stretch fundamental of methanol. J Mol Spectrosc 1991;149:252–6.
[24] Bignall ON, Hunt RH, Shelton WN. Investigation of the torsion rotation energy levels of the CH_3 asymmetric stretches in methanol. J Mol Spectrosc 1994;166:137–46.
[25] Xu L-H, Wang X, Cronin TJ, Perry DS, Fraser GT, Pine AS. Sub-doppler infrared spectra and torsion–rotation energy manifold of methanol in the CH-stretch fundamental region. J Mol Spectrosc 1997;185:158–72.
[26] Villanueva GL, DiSanti MA, Mumma MJ, Xu L-HA. Quantum band model of the ν_3 fundamental of methanol (CH_3OH) and its application to fluorescence spectra of comets. Astrophys J 2012;747:37. http://dx.doi.org/10.1088/0004-637X/747/1/37.
[27] Yaws CL. Chemical properties handbook. McGraw-Hill; 1999.
[28] Harrison JJ, Allen NDC, Bernath PF. Infrared absorption cross sections for acetone (propanone) in the 3 μm region. J Quant Spectrosc Radiat Transfer 2011;112:53–8.
[29] Harrison JJ, Humpage N, Allen NDC, Waterfall AM, Bernath PF, Remedios JJ. Mid-infrared absorption cross sections for acetone (propanone). J Quant Spectrosc Radiat Transfer 2011;112:457–64.
[30] Allen NDC, Harrison JJ, Bernath PF. Acetonitrile (CH_3CN) infrared absorption cross sections in the 3 μm region. J Quant Spectrosc Radiat Transfer 2011;112:1961–6.
[31] Harrison JJ, Bernath PF. Mid- and long-wave infrared absorption cross sections for acetonitrile. J Quant Spectrosc Radiat Transfer 2012;113:221–5.
[32] Sharpe SW, Johnson TJ, Sams RL, Chu PM, Rhoderick GC, Johnson PA. Gas-phase databases for quantitative infrared spectroscopy. Appl Spectrosc 2004;58:1452–61.
[33] Harrison JJ, Allen NDC, Bernath PF. Infrared absorption cross sections for ethane (C_2H_6) in the 3 μm region. J Quant Spectrosc Radiat Transfer 2010;111:357–63. http://dx.doi.org/10.1016/j.jqsrt.2009.09.010.
[34] Breeze JC, Ferriso CC, Ludwig CB, Malkmus W. Temperature Dependence of the Total Integrated Intensity of Vibrational-Rotational Band Systems. J Chem Phys 1965;42:402–6.